Current Research in Food Science 4 (2021) 543–550

Contents lists available at ScienceDirect

Current Research in Food Science

journal homepage: www.sciencedirect.com/journal/current-research-in-food-science

Effects and interaction mechanism of soybean 7S and 11S globulins on anthocyanin stability and antioxidant activity during *in vitro* simulated digestion

Jingyi Zheng [a], Xiuqing Zheng [a], Lei Zhao [b], Junjie Yi [a,*], Shengbao Cai [a,**]

[a] Faculty of Agriculture and Food, Yunnan Institute of Food Safety, Kunming University of Science and Technology, Kunming, 650500, Yunnan, China
[b] Beijing Engineering and Technology Research Center of Food Additives, Beijing Technology and Business University, Beijing, 100048, China

ARTICLE INFO

Keywords:
Anthocyanins
Soybean 7S and 11S Globulins
Stability
Antioxidant activity
Molecular docking
Molecular dynamics simulation

ABSTRACT

The objective of this study was to investigate the effects of soybean 7S and 11S globulins on the stability and antioxidant capacity of cyanidin-3-O-glucoside (C3G) in the simulated gastrointestinal environment, and further to elucidate their interaction mechanism. The stability and total content of anthocyanins (ACNs) before and after simulated digestion were determined by Ultraviolet–visible (UV–Vis) spectroscopic and pH differential methods, respectively, and free radical scavenging activity of C3G after simulated digestion were measured using ABTS and DPPH assays. The interaction mechanism was further investigated using molecular docking and molecular dynamics simulation. The analysis results showed that soybean 7S and 11S globulins had a protective effect on the stability of C3G during simulated digestion and improved the antioxidant capacity of C3G after simulated digestion. Soybean 11S globulin had a better effect than soybean 7S globulin in protecting the stability and antioxidant capacity of C3G against simulated gastrointestinal environment. *In silico* results showed that the binding interactions between C3G and 7S and 11S globulins were mainly hydrogen bonds and van der Waals forces, followed by hydrophobic interactions. Among them, ASN69 and THR101 are the key amino acid residues for 7S–C3G binding, and THR82 and PRO86 are the key amino acid residues for 11S–C3G binding. The results suggested that it may be helpful to use soybean 7S and 11S globulins as carriers to improve the stability and antioxidant activity of ACNs.

1. Introduction

As a kind of natural pigments, anthocyanins (ACNs) are widely found in the cytosol of flowers, fruits, stems, leaves and root organs of plants, giving them different colors ranging from red, purple-red to orchid. ACNs have been shown to have a variety of beneficial health effects and are often used as functional ingredients in the food industry. Recent studies have shown that ACNs possess a variety of biological activities and pharmacological properties such as antioxidant, anti-inflammatory, anti-proliferative, anti-apoptotic and anti-tumor properties *in vitro* and in vivo that protect and promote human health (Dharmawansa, 2020). Valdez and Bolling (2019) found that consumption of ACNs and ACN-rich berries suppressed inflammatory bowel disease in a rodent model of colitis. A recent study reported that ACN inhibited the growth of highly metastatic 4T1 tumor cells and may combat human breast cancer invasion (Silveira et al., 2021). However, ACNs are very unstable in the harsh gastrointestinal environment after oral administration, which is one of the main reasons that cause their low adsorption and bioavailability (Salah et al., 2020). Therefore, it is necessary to improve the stability of ACNs in the gastrointestinal environment and enhance the bioavailability by improving the absorption of ACNs in the digestive tract. It has been shown in several studies that the stability of ACN can be enhanced by interacting with natural polymers and forming complexes (Ren et al., 2021).

Soybean protein isolate (SPI) is a complete high-quality protein whose main components are 7S and 11S globulins (Assad et al., 2020). SPI is known as the only complete protein comparable to animal protein because of its high protein content and digestibility. SPI is often added to processed meat products to increase the protein content, and make the protein in the product more nutritionally sound and complete (Leitner

* Corresponding author.
** Corresponding author.
E-mail addresses: junjieyi@kust.edu.cn (J. Yi), caikmust2013@163.com, caikmust2013@kmust.edu.cn (S. Cai).

https://doi.org/10.1016/j.crfs.2021.08.003
Received 12 July 2021; Received in revised form 4 August 2021; Accepted 10 August 2021
Available online 13 August 2021

et al., 2006). In addition, SPI has excellent properties and the potential for encapsulation and delivery of active substances. It was shown that quercetin can bind to the hydrophobic capsule of SPI particles through hydrophobic interaction and hydrogen bonding, and SPI particles can act as a protective carrier for quercetin (Meng et al., 2017). Ju et al. (2019) successfully prepared novel picolin emulsions stabilized by SPI-acrylonitrile composite nanoparticles as a protective mechanism to prolong the stability of oxidizable lipids and lipid-soluble nutrients. Several recent studies have shown that protein-ACN interactions alter the structure, antioxidant activity, stability, and *in vitro* digestibility of proteins (Jian et al., 2019; Ren et al., 2019). Zang et al. (2020) found that whey isolate protein trapped blueberry ACNs within its protein cavity, leading to its slow degradation thereby improving the stability and antioxidant capacity of ACNs. It has also been shown that the strong binding affinity between preheated SPI and C3G affected the secondary structure of SPI, which can effectively protect the stability of C3G (Chen et al., 2019). However, previous studies only focused on the effect of SPI on the stability and antioxidant activity of ACNs, and the effect of soybean 7S and 11S globulins on the stability and antioxidant activity of the ACNs has not been clearly studied.

In this study, C3G was selected as the representative of ACNs. The effects and action of mechanism of soybean 7S and 11S globulins on the stability and antioxidant capacity of C3G in the simulated gastrointestinal environment were investigated. The changes in the concentration of C3G after simulated digestion were determined by using spectral methods. Molecular docking combined with molecular dynamics simulation analyses were used to reveal the interactions between C3G and soybean 7S and 11S globulins. This study will provide valuable information for the development and application of functional soybean-based beverage products.

2. Materials and methods

2.1. Chemicals and reagents

Defatted soybean flour was obtained from Zhaoyuan Wenji Food Co., Ltd (Yantai, Shandong, China) with 40% protein content. 2-Diphenyl-1-picryhydrazyl (DPPH) radical, 2,2′-azino-bis(3-ethyl-benzothiazoline-6-sulfonic acid) (ABTS), pepsin from porcine gastric mucosa (3860 units/mg protein) (EC 3.4.23.1), pancreatin from porcine pancreas (8 × USP specifications), and bile salts were purchased from Sigma-Aldrich (Shanghai, China). Authentic standard of cyanidin-3-*O*-glucoside (C3G) (purity ≥98%) was obtained from Chengdu Must Biotechnology Co., Ltd (Chengdu, Sichuan, China).

2.2. Preparation of soybean 7S and 11S globulins

The protein was prepared based on the published method of Liu et al. (2007) with slight modifications. Ten grams of low temperature defatted soybean powder was dissolved with 15 times volume of distilled water, and adjusted pH to 9.0 with 2 mol/L sodium hydroxide. The mixture was extracted twice in a water bath at 45 °C for 1 h with low speed stirring, and then centrifuged at 9000×*g* for 20 min. The concentration of supernatant was adjusted to 0.01 mol/L with solid $NaHSO_3$, and adjusted pH to 6.4 with 2 mol/L HCl. After storing at 4 °C overnight, the precipitate obtained by centrifugation (6500×*g*, 20min, 4 °C) was washed twice with distilled water, dissolved with distilled water, adjusted pH to 7.5, and freeze-dried to give 11S components. The supernatant was adjusted to a concentration of 0.25 mol/L with solid NaCl and adjusted to pH 4.8 with 2 mol/L HCl, and then centrifuged (6500×*g*, 20 min, 4 °C). The precipitate was washed twice with distilled water and then dissolved with distilled water, adjusted pH to 7.5, and freeze-dried to give 7S components. After detecting the purity of 7S and 11S globulins by SDS-PAGE, the protein concentration was determined by BCA method, and the concentrations of soybean 7S and 11S globulins were calculated to be 975.33 μg/mL and 6078 μg/mL, respectively.

2.3. In vitro simulated digestion process

In vitro simulated digestion experiments were performed based on the existing methods (Liu et al., 2020). In this experiment, a control group (CG), a simulated gastric digestion group (GD) and a simulated intestinal digestion group (ID) were established. All the solutions were prepared with 0.05 mol/L phosphate buffer solution (pH 3). A total of 5 mL of 0.05 mg/mL soybean 7S and 11S globulin solutions were mixed with 5 mL of 32 μmol/L C3G, respectively, and the mixtures of GD and ID groups were adjusted to pH 3 with 1 mol/L HCl. Afterwards, 0.17 mL of pepsin solution was added to each of the two groups (0.6 g of pepsin in 10 mL of 0.1 mol/L HCl). All mixtures (CG, GD and ID groups) were incubated on a shaker (200 rpm, 37 °C) in the dark for 2 h. After incubation, the supernatant of the GD group was collected as a GD sample (pH 3) by centrifugation at 8000×*g* for 15 min at 4 °C, and the pH of ID group was changed to 7.5 with 1 mol/L $NaHCO_3$. The mixture of ID group was then added to 1.7 mL of trypsin and bile salt solution (0.5 g trypsin, 1.2 g bile salt in 0.1 mol/L $NaHCO_3$ solution). After that, the mixtures of CG and ID groups were further incubated in a shaker for 2 h. Finally, the pH values of the CG and ID groups were adjusted to pH 3. Then, the mixtures were separated by centrifugation and the supernatants were collected as CG and ID samples, respectively. Finally, the supernatants of CG and GD groups were added with phosphate buffer salt solution, and the samples of CG, GD and ID groups were in the same volume for subsequent comparative experiments.

2.4. Ultraviolet–visible (UV–Vis) spectroscopic analysis and the spectrophotometric pH differential method

The stability of ACNs was determined by measuring the absorbance of non-digested and *in vitro* digested samples at pH 3 in the wavelength range of 200–800 nm at 10 nm intervals. The total ACN content was determined using the pH differential method, as reported in the literature with slight modifications (Sun et al., 2015). Briefly, each sample was diluted with potassium chloride buffer (0.03 mol/L, pH 1.0) and sodium acetate buffer (0.4 mol/L, pH 4.5) buffers to attain the same dilution. The absorbance was measured at 520 nm and 700 nm, respectively, using a UV spectrophotometer. The blank group was made in three parallel groups with 1 mL of phosphate buffer solution added to 9 mL of buffer solution. The formula of total ACN concentration (mg/L) = (A × MW × DF × 103)/(ε × L), where $A = (A_{520}\text{-}A_{700})_{pH1.0}\text{-}(A_{520}\text{-}A_{700})_{pH4.5}$, MW = 449.38 g/mol, D is the dilution factor, which is 2-fold in this experiment, ε is the extinction coefficient 26900 L/mol/cm, and L is the path length of 1 cm.

2.5. Evaluation of antioxidant activity

2.5.1. DPPH radical scavenging activity

The DPPH radical scavenging ability of non-digested and *in vitro* digested samples was determined with reference to the published method of Yang et al. (2021). The samples were dissolved in methanol and gradient diluted to five different concentrations of 50 μg/mL, 100 μg/mL, 150 μg/mL, and 200 μg/mL, respectively. For each group, 2 mL of DPPH and 0.5 mL of sample were mixed and shaken for 30 min in the dark. The same volumes of distilled water and methanol were added and the reaction was performed under the same conditions for zeroing. After the reaction, the absorbance values of each group were recorded at 517 nm, and the scavenging rate of each group was calculated according to the formula: DPPH radical scavenging rate (%) = (absorbance value of control group - absorbance value of sample group)/absorbance value of control group lated accordin experiment, the *in vitro* digested samples of C3G without protein addition were used as positive control, and the corresponding DPPH scavenging ability was measured under the same conditions.

2.5.2. ABTS radical cation scavenging activity

The ABTS radical cation scavenging ability of non-digested and *in vitro* digested samples was determined by referring to the published method (Liu and Ning, 2021). The samples were dissolved in methanol and gradient diluted to five different concentrations of 50 μg/mL, 100 μg/mL, 150 μg/mL, and 200 μg/mL, respectively. For each group, 4 mL of ABTS and 0.5 mL of sample were added to each assay group, and a water bath at 30 °C for 6 min in the dark. The reaction was performed under the same conditions for zeroing by adding the volume of ethanol and the volume of distilled water of the sample. After cooling to room temperature, the absorbance values of each group were recorded at 734 nm, and the scavenging rate of each group was calculated according to the formula: ABTS radical cation scavenging rate (%) = (absorbance value of control group - absorbance value of sample group)/absorbance value of control group × 100. In this experiment, the *in vitro* digested samples of C3G without protein addition were used as positive control, and the corresponding ABTS radical cation scavenging ability was measured under the same conditions.

2.6. Molecular docking

Soybean 11S and 7S globulins with known intact structures were selected and docked with C3G. 3D model of C3G was downloaded from the PubChem database (http://PubChem.ncbi.nlm.nih.gov) with registration number 197081 and was optimized using sybly-xy2.1 software as ligand. Soybean 11S globulin (PDB-ID: 1OD5) and 7S globulin (PDB-ID: 3AUP) files were downloaded from the PDB database (http://www.rcsb.org/pdb/home/home.do) as receptors and docked under SYBLY software. Molecular docking was performed using high precision mode (SFXC). Before docking, the structures of each protein were pretreated to remove water molecules, metal ions and their own ligands, and then the proteins were hydrogenated and charged to expose their active pockets. Finally, the proteins were molecularly docked with small molecule ligands, and the conformational docking with the highest docking T-score was selected.

2.7. Molecular dynamics simulation

SYBYL molecular docking offers the possibility to find the best binding conformation of the C3G-7S and C3G-11S complexes. However, this approach cannot analyze the binding stability between compounds. Therefore, we performed 100 ns MD simulations of the C3G-7S, C3G-11S, 7S and 11S systems using the GROMACS 19.6 package with Amber99sb-ildn force field and TIP3P explicit water model. Counter ions were added to meet the electrical neutrality of the systems. Then, constant temperature and pressure of the complex system was achieved by energy minimization (steepest drop of 1000.0 kJ mol^{-1} nm^{-1}), NVT (310.15 K, 500 ps) and NPT (1.0 bar, 1000 ps) simulations. Among them, the V-rescale and Parrinello-Rahman schemes are used to control the temperature and pressure of the complex system, respectively. After the MD simulations, the trajectories were analyzed using GROMACS (Van Der Spoel et al., 2005) and the energy decomposition of the complexes was performed using the GMX_MMPBSA tool (https://github.com/Jerkwin/gmxtool/tree/master/gmx_mmpbsa).The results of MD simulations can explain the conformational and energetic changes of C3G and protein complexes during the binding process and further provide a basis for the mechanism of C3G binding action with soybean 7S and 11S globulins.

2.8. Statistical analysis

All data are expressed as the mean values ± standard deviation (SD). Normal distribution of residuals was examined using SPSS 20.0 (SPSS, Inc., Chicago, IL, USA). Homogeneity of variance and one-way analysis of variance (one-way ANOVA) of all data were performed with Origin 2019b (OriginLab, Northampton, MA, USA). Normal distribution of residuals and homogeneity of variance were achieved for data. Tukey's procedure was used for analyzing the significance of difference ($p < 0.05$, different significantly).

3. Results and discussion

3.1. The effect of soybean 7S and 11S globulins on the stability of C3G

The changes in spectral characteristics reflect the stability of C3G during gastrointestinal digestion. As shown in Fig. 1, there were some differences in the UV–Vis spectrogram of undigested, gastric digested and intestinal digested samples of the C3G-7S, C3G-11S groups and the C3G group without protein, indicating that the chemical structure of C3G changed somewhat during the *in vitro* simulated digestion. There were two characteristic absorption peaks of ACN at 260 nm and 520 nm. The UV–vis spectra of C3G in the presence and absence of soybean proteins after simulated gastric digestion were not much different from those of the undigested samples (Fig. 1). However, the absorbance value at 520 nm of the C3G group without soybean proteins decreased significantly by about 51.5% after intestinal digestion, indicating that the C3G was unstable and degraded under intestinal conditions (Fernandes et al., 2017). The results suggested that C3G is more stable in acidic or neutral environments and easily degraded in high pH solution environments. As can be seen in Fig. 1, after simulated intestinal digestion, the absorbance of the C3G-7S group at 520 nm decreased by about 39.4%, and the absorbance of the C3G-11S group here also decreased by about 37.2%. The absorbance of the C3G-7S and C3G-11S groups at 520 nm were higher than that of the C3G group without protein. It indicated that soybean proteins have a protective effect on the stability of C3G against simulated intestinal digestion, and the soybean 11S protein has a somewhat better protective effect compared to soybean 7S proteins.

The pH differential method was used to determine the total C3G content in undigested and digested samples, and the effects of soybean 7S and 11S globulins on the C3G concentration after *in vitro* simulated digestion are shown in Table 1. The stability of C3G during simulated digestion can be expressed by the change in retention rate - the higher the retention rate, the better the stability of C3G. As the intestinal digestion proceeded, a gradual decrease in C3G levels from gastric to intestinal digestion could be observed in the control group, and approximately 75.6% of the total C3G content was degraded, which is consistent with previous studies (Sun et al., 2015). In the gastric phase, there was no significant difference in the C3G concentration between groups with or without 7S and 11S globulins. After intestinal digestion, the C3G concentrations in the C3G, C3G-7S and C3G-11S groups significantly decreased to 2.88 ± 0.06, 3.28 ± 0.11 and 3.46 ± 0.17 mg/L, respectively. This indicates that C3G remained stable during gastric digestion but not during intestinal digestion. The weak alkaline environment of the small intestine may be the main reason for the decrease in C3G content during intestinal digestion (Liu et al., 2014). The retention rate of C3G without protein was slightly lower than those of the C3G groups with protein protection. These results indicated that soybean 7S and 11S globulins had a certain protective effect on C3G against gastrointestinal digestion, and the protection effect of soybean 11S globulin was slightly better than that of soybean 7S globulins, which was consistent with the UV–Vis scanning results.

3.2. Stability of antioxidant activities of C3G influenced by soybean 7S or 11S globulins

The DPPH radical scavenging rates and ABTS radical cation scavenging rates of the C3G-7 and C3G-11S complex groups were subtracted from the corresponding scavenging rates of their soybean 7S and 11S globulin groups without C3G samples before and after simulated digestion to exclude the interference of soybean 7S and 11S globulins and protein-produced peptides on the antioxidant assay of their C3G

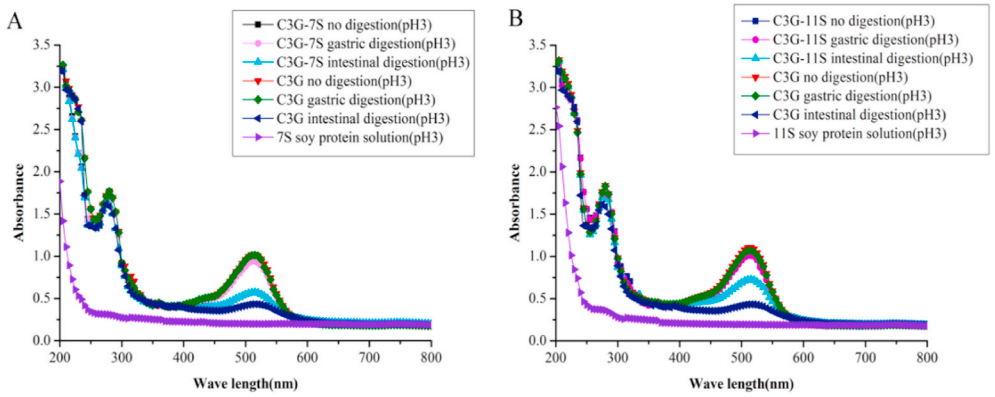

Fig. 1. UV–vis spectral features of C3G before and after *in vitro* simulated digestion in the presence of soybean 7S **(A)** and 11S **(B)** globulins.

Table 1
Changes in concentration of total cyanidin-3-O-glucoside (C3G) before and after *in vitro* gastrointestinal digestion in the absence and presence of soybean 7S and 11S globulins.

Total C3G (mg/L)	C3G-7S	C3G-11S	C3G
No digestion	8.39 ± 0.44^{Ab}	8.58 ± 0.43^{Ab}	8.03 ± 0.29^{Ab}
Gastric digestion	9.05 ± 1.37^{Ab}	9.19 ± 1.20^{Ab}	8.29 ± 0.25^{Ab}
Intestinal digestion	3.04 ± 0.11^{Ba}	3.21 ± 0.17^{Ba}	2.67 ± 0.06^{Aa}

C3G-7S: mixture of C3G and soybean 7S globulin; C3G-11S: mixture of C3G and soybean 11S globulin. In the same column, significant differences are indicated by different superscript lowercase letters ($p < 0.05$). In the same row, significant differences are indicated by different superscript capital letters ($p < 0.05$).

samples after simulated digestion.

ACNs are relatively stable during simulated gastric digestion, and the protection of ACNs should focus on the intestinal digestion process since the alkaline environment of the intestine is the main cause of ACN degradation and poor accessibility (Lang et al., 2020). As shown in Table 2, when the samples were digested in the simulated intestinal juice for 2 h, the IC_{50} values for the DPPH radical scavenging capacities of the control, C3G-7S and C3G-11S groups were 74.94 ± 3.01, 65.8 ± 0.50 and 56.3 ± 0.46 μg/mL, respectively. The samples from the C3G-7S and C3G-11S groups showed significantly lower IC_{50} values of the scavenging activities of DPPH radical than that of the control group ($p < 0.05$). These results suggest that the addition of soybean 7S and 11S globulins improved the antioxidant activity of C3G itself during simulated intestinal digestion. As shown in Table 3, during the whole simulated digestion, the ABTS radical cation scavenging activities of the C3G-11S and C3G-7S groups were stronger than that of the control group at almost all tested concentrations. The IC_{50} values of the ABTS radical cation scavenging activities in the C3G-11S, C3G-7S and control groups after 2 h of simulated intestinal digestion were 37.39 ± 1.65 μg/mL, 47.56 ± 1.12 μg/mL and 68.94 ± 1.35 μg/mL, respectively. The IC_{50} values of the ABTS radical cation scavenging capacities of the C3G-11S and C3G-7S groups were significantly lower than that of the control group ($p < 0.05$). The results showed that soybean 7S and 11S globulins improved the antioxidant capacity of C3G during gastrointestinal digestion, and soybean 11S globulin was somewhat more effective than soybean 7S globulin in improving the antioxidant capacity of C3G.

3.3. Molecular docking of C3G-soybean 7S and 11S globulins complexes

The interactions between macromolecules and ligands can be quickly and easily known by molecular docking methods. The docking results of C3G-7S and C3G-11S with their highest T-scores of 4.6904 and 4.7904, respectively, were selected for further study. As shown in Fig. 2 a1, a2 and b1, b2, C3G can be tightly bound to soybean 7S and 11S globulins,

Table 2
DPPH radical scavenging activities of cyanidin-3-O-glucoside (C3G) in the absence and presence of soybean 7S and 11S globulins before and after *in vitro* simulated digestion.

In vitro digestion procedures	Concentrations (μg/mL)	C3G	C3G-7S	C3G-11S
No digestion	20	14.45 ± 0.30ABa	13.82 ± 0.15Aa	17.08 ± 0.16Ba
	40	20.68 ± 0.18Bb	13.03 ± 2.31Aa	19.47 ± 0.73Ba
	60	34.30 ± 2.00Ac	28.81 ± 2.02Ab	36.22 ± 0.94Bb
	80	42.17 ± 1.80Ad	36.85 ± 1.09Ac	50.01 ± 2.71Bc
	100	50.49 ± 1.85Ae	57.76 ± 1.78Bd	67.33 ± 0.33Cd
Gastric digestion	20	12.39 ± 2.00Aa	14.61 ± 0.99Aa	19.07 ± 1.40Ba
	40	21.44 ± 1.50Ab	28.95 ± 2.96Bb	30.28 ± 1.83Bb
	60	34.53 ± 2.98Ac	37.57 ± 0.98ABc	37.79 ± 1.92Bc
	80	52.97 ± 0.91Ad	54.58 ± 0.97Ad	51.79 ± 2.52Ad
	100	63.08 ± 2.97Ae	70.47 ± 1.10Be	70.91 ± 2.22Be
Intestinal digestion	20	16.94 ± 1.05Aa	16.52 ± 0.54Aa	26.60 ± 1.46Ba
	40	22.66 ± 1.16Ab	30.31 ± 0.25Bb	37.09 ± 1.44Cb
	60	44.30 ± 1.59Ac	47.35 ± 1.38Ac	54.49 ± 1.46Bc
	80	57.75 ± 2.42Ad	57.83 ± 0.39Ad	60.67 ± 1.59Ad
	100	69.39 ± 2.57Ae	76.75 ± 1.30Be	83.96 ± 1.65Ce

C3G-7S: mixture of C3G and soybean 7S globulin; C3G-11S: mixture of C3G and soybean 11S globulin. In the same column, at different concentrations with the same *in vitro* digestion process, significant differences are indicated by different superscript lowercase letters ($p < 0.05$). In the same row, significant differences of the different groups are indicated by different superscript capital letters ($p < 0.05$).

and the amino acid binding pockets of soybean 7S and 11S globulins can wrap around C3G, thus producing a protective effect on C3G and thus improving the stability of C3G. Lang et al. (2019) found that ACN can enter and be surrounded by bovine serum albumin using molecular docking analysis, thus providing protection against blueberry ACN (Lang et al., 2019).

As shown in Fig. 2, the molecular docking hydrogen bonding diagram of the C3G-7S and C3G-11S complexes indicated that the hydroxyl hydrogen atom on C3G can bind between the active site on the protein via hydrogen bonding (yellow dashed line). Hydrogen bonding is one of

Table 3
ABTS radical scavenging activities of cyanidin-3-O-glucoside (C3G) in the absence and presence of soybean 7S and 11S globulins before and after *in vitro* simulated digestion.

In vitro digestion procedures	Concentrations (μg/mL)	C3G	C3G-7S	C3G-11S
No digestion	20	9.87 ± 2.98Aa	23.02 ± 2.38Ba	23.32 ± 2.63Ba
	40	20.92 ± 3.33Ab	25.75 ± 0.36ABa	29.76 ± 1.82Ba
	60	32.84 ± 2.26Ac	37.99 ± 1.12Ab	49.35 ± 1.14Bb
	80	48.69 ± 2.76Ad	55.36 ± 2.80Bc	71.24 ± 1.33Cc
	100	70.26 ± 1.96Ae	71.12 ± 2.06Ad	79.31 ± 2.16Bd
Gastric digestion	20	9.73 ± 0.40Aa	24.59 ± 1.54Ba	31.12 ± 0.35Ca
	40	30.33 ± 0.65Ab	32.44 ± 0.98Ab	50.21 ± 0.31Bb
	60	38.22 ± 1.14Ac	45.75 ± 0.44Bc	64.14 ± 0.26Cc
	80	60.19 ± 1.54Ad	64.76 ± 0.67Ad	72.93 ± 0.21Bd
	100	71.28 ± 4.36Ae	73.96 ± 1.38Ae	84.00 ± 1.51Be
Intestinal digestion	20	13.20 ± 1.22Aa	25.63 ± 3.54Ba	36.25 ± 3.10Ca
	40	39.94 ± 0.66Ab	51.72 ± 3.96Bb	53.90 ± 2.25Bb
	60	49.57 ± 0.21Ac	62.48 ± 3.45Bc	65.91 ± 1.63Bc
	80	63.99 ± 2.37Ad	67.10 ± 1.91Ac	77.91 ± 3.81Bd
	100	76.46 ± 1.48Ae	84.95 ± 3.09Bd	89.22 ± 0.55Be

C3G-7S: mixture of C3G and soybean 7S globulin; C3G-11S: mixture of C3G and soybean 11S globulin. In the same column, at different concentrations with the same *in vitro* digestion process, significant differences are indicated by different superscript lowercase letters ($p < 0.05$). In the same row, significant differences of the different groups are indicated by different superscript capital letters ($p < 0.05$).

the most important intermolecular interactions between molecules (Munawaroh et al., 2020). C3G formed four hydrogen bonds with the active pocket of soybean 7S globulin with an average hydrogen bond distance of 2.040 Å. The action sites included four amino acid residues HIS23, VAL40, LEU161 and ALA363. C3G formed four hydrogen bonds with the active pocket of soybean 11S globulin with an average hydrogen bond distance of 2.225 Å. The action sites included four amino acid residues LEU374, LEU422, LEU439 and VAL442. The analysis revealed that the interactions between C3G and soybean 7S and 11S globulins include hydrogen bonding and hydrophobic interactions. Ren et al. (2019) inferred that hydrophobic forces play a role in the binding of C3G to soybean 7S and 11S globulins by isothermal titration thermal analysis. It has also been reported that preheated silkworm pupae protein (SPP) improved on the stability of C3G during food processing, which is due to the hydrophobic interaction between C3G and preheated SPP complexes (Attaribo et al., 2020). Thus, hydrophobic interactions play an important role in the protection of the stability of soybean 7S and 11S globulins during simulated digestion.

3.4. Molecular dynamics (MD) simulation results

The addition of various common food biopolymers such as whey protein (WP), β-cyclodextrin (β-CD) and soy protein (SP) is an effective way to improve the stability of ACNs. The protective effects and mechanisms of action of these food biopolymers on ACNs are different from each other (Chung et al., 2015; Fernandes et al., 2017; Sui et al., 2018). Molecular dynamics simulations were performed to better understand the interaction mechanism between C3G ligands and soybean 7S and 11S globulin receptors, and to further validate the above experimental results at the molecular level. The root mean square deviation (RMSD) is a key indicator of whether the simulated system is in equilibrium (Liu and Ning, 2021). Throughout the MD simulation, the RMSD changes of receptor 7S and complex 7S -C3G are shown in Fig. 3A. The RMSD values of receptor 7S and complex 7S–C3G showed a general trend of gradual increase within 100 ns, and the RMSD tended to flatten out after 70 ns of MD simulation, indicating that the two systems had reached equilibrium. The RMSD values of both receptor 11S and complex 11S–C3G gradually increased during the first 30 ns, declined rapidly after 30 ns, and gradually increased near 40 ns. The fluctuations were less towards the end of the simulation, indicating that the structures of receptor 11S and complex 11S–C3G were changed in the new environment. As shown in Fig. 3B, a Gaussian function was used to integrate the RMSD values, and the probability of distribution of RMSD was used as the vertical coordinate, and the normal distribution was presented in the form of a plot. The distance of complex 7S–C3G was concentrated between 0.25 nm and 0.35 nm, and the maximum probability of distribution was nearly 32%. The distance of receptor 7S globulin was concentrated between 0.15 nm and 0.35 nm, which was more extensive than that of complex 7S–C3G, and the maximum distribution probability is less than 22.5%. It can be seen that the complex 7S–C3G have a tighter distance distribution compared to the receptor 7S. Compared with the receptor 7S, the complex 7S–C3G system is more

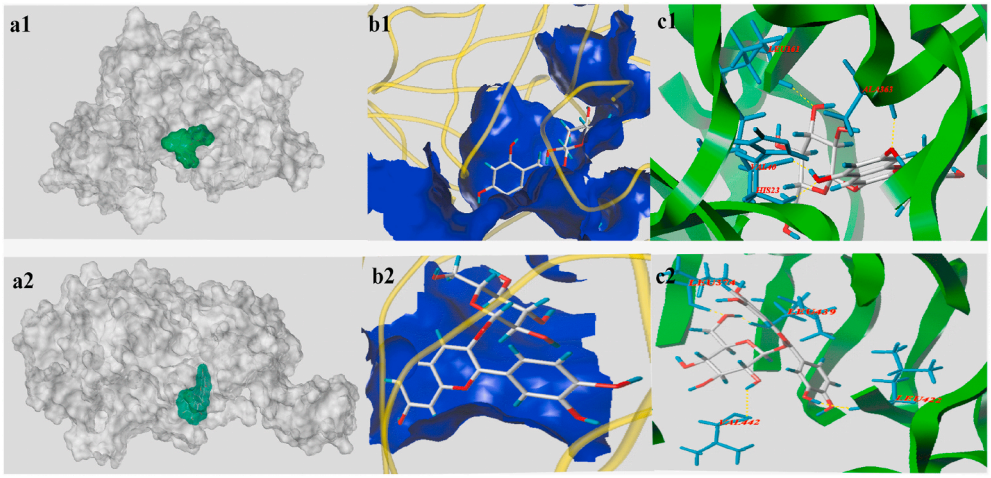

Fig. 2. Binding modes of cyanidin-3-O-glucoside (C3G) to soybean 7S and 11S globulins by molecular docking. **(1)** C3G-7S, **(2)** C3G-11S. Letters a-b represent the binding sites, binding pockets and binding hydrogen bonding diagrams between C3G and soybean 7S and 11S globulins, respectively.

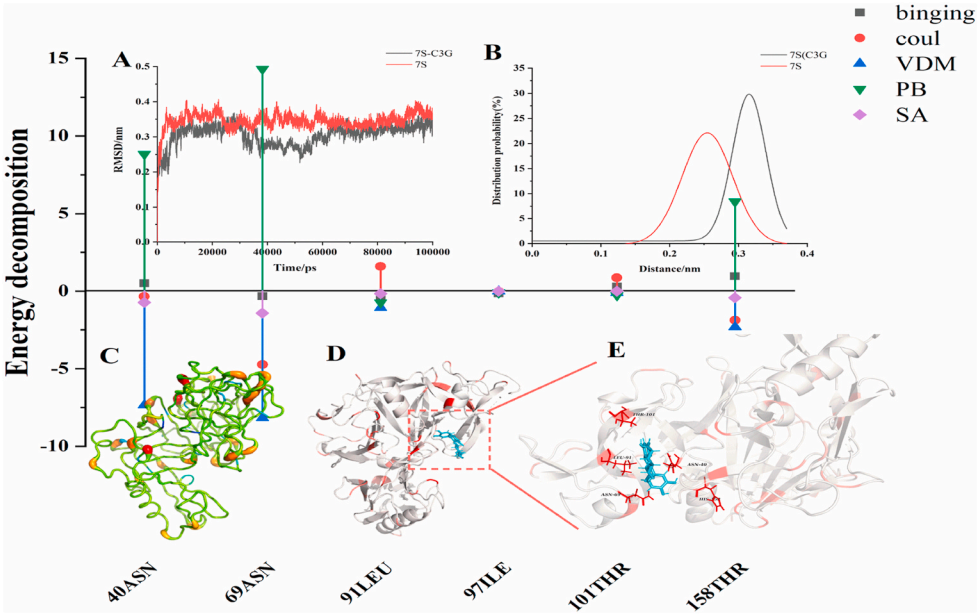

Fig. 3. The per-residue energy contribution spectrums of the complex C3G-7S. **(A)** RMSD values of the protein backbone for 7S (red) and 7S–C3G complex systems (black) during MD simulations. **(B)** Plot of RMSD Gaussian function integral normal distribution. **(C)** Plot of the total contribution of each amino acid of soybean 7S globulin to the binding energy. **(D)** Interaction diagram. **(E)** Critical residues for binding. (For interpretation of the references to color in this figure legend, the reader is referred to the Web version of this article.)

stable. As shown in Fig. 4A, the RMSD values of receptor 11S and complex 11S–C3G showed a general trend of gradual and slow increase with time. MD simulation after 65 ns RMSD gradually flattens out the system has reached equilibrium. As shown in Fig. 4B, the distance of the normal distribution plot of complex 11S–C3G were concentrated between 0.40 nm and 0.70 nm, and the probability of the maximum distribution was nearly 34%. The distance of receptor 11S is concentrated between 0.30 nm and 0.70 nm, and the distribution is a little wider than that of complex 11S–C3G, with a maximum distribution probability of less than 32%. It can be seen that the distribution of the distance of complex 11S–C3G are not very different from that of receptor 11S, but in general, the system stability of complex 11S–C3G are a little better than that of receptor 11S.

Fig. 3 (C, D and E) and Fig. 4 (C, D and E) show the extraction of amino acid residues in the range of 5 Å around the C3G ligand, and then the energy contributions of various amino acid residues were decomposed and analyzed, including the binding energy, Poisson-Boltzmann surface area (PBSA) energy contribution, solvent accessible surface area (SASA) energy contribution, Coulomb force and van der Waals force. SASA can be used to describe the tightness of proteins, and PB is a free energy calculation based on adequate MD sampling. The EBind value between C3G and 7S was 54.49 kJ/mol, where ESASA, ECoul, EPB, and EVdw values were −18.69 kJ/mol, 55.60 kJ/mol, 139.48 kJ/mol, and −121.90 kJ/mol, respectively. And the EBind value between C3G and 11S is −572.02 kJ/mol, where ESASA, ECoul, EPB and EVdw values were −20.61 kJ/mol, -592.12 kJ/mol, 196.60 kJ/mol, −155.89 kJ/mol respectively.

Fig. 3C and Fig. 4C show the total contribution of each amino acid to the binding energy, and their average values were taken for the graphical analysis. The thickness of the lines in the graph indicates the size of

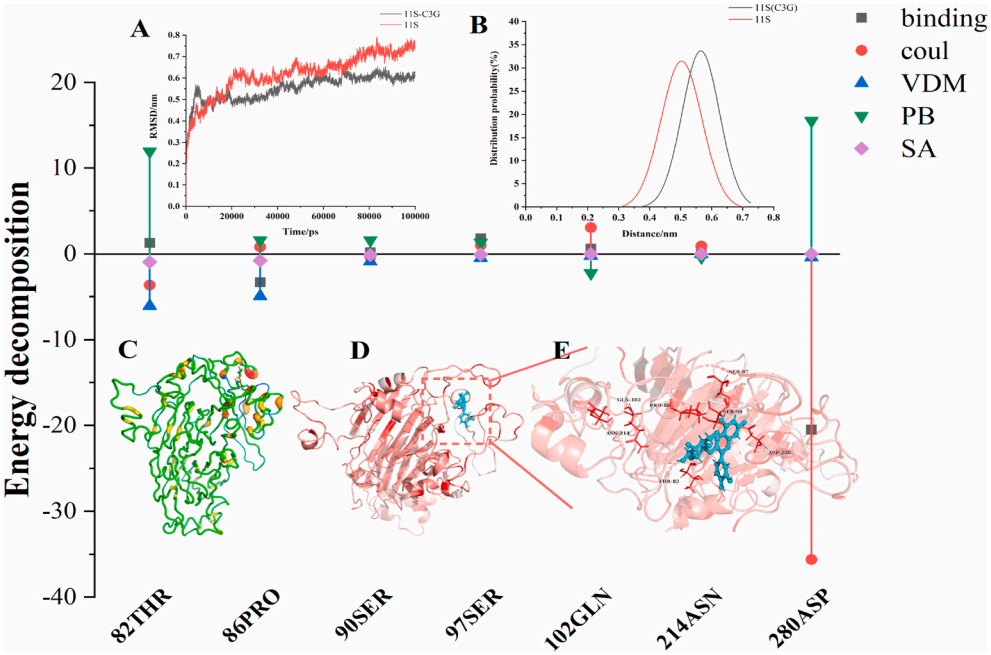

Fig. 4. The per-residue energy contribution spectrums of the complex C3G-11S. **(A)** RMSD values for the protein backbone of 11S (red) and 11S–C3G complex systems (black) during MD simulations. **(B)** Plot of RMSD Gaussian function integral normal distribution. **(C)** Plot of the total contribution of each amino acid of soybean 11S globulin to the binding energy. **(D)** Interaction diagram. **(E)** Critical residues for binding. (For interpretation of the references to color in this figure legend, the reader is referred to the Web version of this article.)

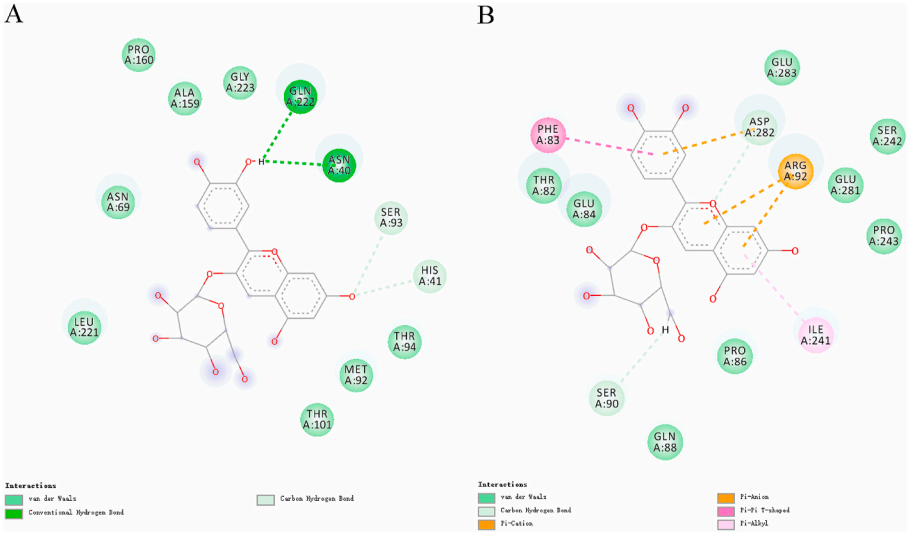

Fig. 5. 2D diagram of interaction between C3G and soybean 7S **(A)** and 11S **(B)** globulins.

the contribution of the amino acid residue to EBind. The thicker line and the darker color of the amino acid residue were, the greater the contribution of that amino acid residue was to EBind. The results showed that the binding pocket contributed a lot to the binding energy of C3G. To further understand the contribution of each amino acid residue, EBind was calculated. As shown in Fig. 3D and Fig. 3E, the residues of 7S interacting with C3G were mainly ASN40, ASN69, ILE97, THR101, and THR158. As shown in Fig. 4D and Fig. 4E, the residues of 11S interacting with C3G are mainly THR82, PRO86, SER97, and ASP280. These residues contribute the major binding energy of the binding region (absolute value $>$ 2 kJ/mol) in the binding region. Discovery Studio 2016 client analysis are presented in Fig. 5. The results showed that C3G interacted with the amino acid residues in the binding pocket of 7S through hydrogen bonds (ASN40, HIS41, SER93 and GLN222) and van der Waals forces (ASN69, MET92, THR94, THR101, ALA159, PRO160 and LEU221). The interactions of C3G with the amino acid residues in the binding pocket of 11S were hydrogen bonding (SER90 and ASP282), van der Waals forces (THR82, GLU84, PRO86 and GLN88, SER242, PRO243, GLU281 and GLU283), and hydrophobic interactions (both alkyl and pi-alkyl).

4. Conclusions

The protective effect of soybean 7S and 11S globulins on C3G was investigated under simulated digestion conditions. C3G was stable in the gastric environment and was easy to degrade in the intestinal environment. Soybean 7S and 11S globulins protected the stability of C3G during intestinal digestion and improved the antioxidant capacity of C3G, and soybean 11S globulin was better than soybean 7S globulin in terms of protection and improving the antioxidant capacity of C3G. The interactions between C3G and soybean 7S and 11S globulins were mainly hydrogen bonds and van der Waals forces, followed by hydrophobic interactions. Among them, ASN69 and THR101 were the key amino acid residues for 7S–C3G binding, and THR82 and PRO86 were the key amino acid residues for 11S–C3G binding. The results of this study may provide a basis for further application of soybean 7S and 11S globulins as microcapsule carriers to protect the stability and antioxidant activity of ACNs and expand the application of ACNs as stable and functional food ingredients.

CRediT authorship contribution statement

Jingyi Zheng: Investigation, Data curation, Writing – original draft. **Xiuqing Zheng:** Data curation, Writing – original draft. **Lei Zhao:** Methodology, Writing – review & editing. **Junjie Yi:** Writing – review & editing, Funding acquisition, Supervision. **Shengbao Cai:** Conceptualization, Methodology, Supervision, Funding acquisition.

Declaration of competing interest

The authors declare that they have no known competing financial interests or personal relationships that could have appeared to influence the work reported in this paper.

Acknowledgments

The present work was financially supported by the National Natural Science Foundation of China (Grant Nos. 31901711 and 31960477), Science and Technology Project of Yunnan Province (Nos. 202002AE320006-01-03 and 2019ZG001-4-1) and Key Research and Development Program of Kunming City (No. 2019-1-N-25318000003141).

References

Assad, I., Bhat, S.U., Gani, A., Shah, A., 2020. Protein based packaging of plant origin: fabrication, properties, recent advances and future perspectives. Int. J. Biol. Macromol. 164, 707–716. https://doi.org/10.1016/j.ijbiomac.2020.07.140.

Attaribo, T., Jiang, X., Huang, G., Zhang, B., Gui, Z., 2020. Studies on the interactional characterization of preheated silkworm pupae protein (SPP) with anthocyanins (C3G) and their effect on anthocyanin stability. Food Chem. 326, 126904. https://doi.org/10.1016/j.foodchem.2020.126904.

Chen, Z., Wang, C., Gao, X., Chen, Y., Santhanam, R.K., Wang, C., Xu, L., Chen, H., 2019. Interaction characterization of preheated soy protein isolate with cyanidin-3-O-glucoside and their effects on the stability of black soybean seed coat anthocyanins extracts. Food Chem. 271, 266–273. https://doi.org/10.1016/j.foodchem.2018.07.170.

Chung, C., Rojanasasithara, T., Mutilangi, W., Mcclements, D.J., 2015. Enhanced stability of anthocyanin-based color in model beverage systems through whey protein isolate complexation. Food Res. Int. 76, 761–768. https://doi.org/10.1016/j.foodres.2015.07.003.

Dharmawansa, K., 2020. Dietary anthocyanins-smart molecules with chemo preventive and chemotherapeutic activity. Org. Med. Chem. Int. J. 10, 23–26. https://doi.org/10.19080/OMCIJ.2020.10.555779.

Fernandes, A., Rocha, M.A.A., Santos, L.M.N.B.F., Brás, J., Oliveira, J., Mateus, N., de Freitas, V., 2017. Blackberry anthocyanins: β-Cyclodextrin fortification for thermal and gastrointestinal stabilization. Food Chem. 245, 426–431, 10.1016/j.foodchem.2017.10.109.

Jian, L., Liu, Y., Li, L., Qi, B., Ju, M., Xu, Y., Yan, Z., Sui, X., 2019. Covalent conjugates of anthocyanins to soy protein: unravelling their structure features and in vitro gastrointestinal digestion fate. Food Res. Int. 120, 603–609. https://doi.org/10.1016/j.foodres.2018.11.011.

Ju, M., Zhu, G., Huang, G., Shen, X., Sui, X., 2019. A novel pickering emulsion produced using soy protein-anthocyanin complex nanoparticles. Food Hydrocolloids 99, 105329. https://doi.org/10.1016/j.foodhyd.2019.105329.

Lang, Y., Li, B., Gong, E., Shu, C., Si, X., Gao, N., Meng, X., 2020. Effects of α-casein and β-casein on the stability, antioxidant activity and bioaccessibility of blueberry anthocyanins with an in vitro simulated digestion. Food Chem. 334, 127526. https://doi.org/10.1016/j.foodchem.2020.127526.

Lang, Y., Li, E., Meng, X., Tian, J., Ran, X., Zhang, Y., Zang, Z., Wang, W., Li, B., 2019. Protective effects of bovine serum albumin on blueberry anthocyanins under illumination conditions and their mechanism analysis. Food Res. Int. 122, 487–495. https://doi.org/10.1016/j.foodres.2019.05.021.

Leitner, A., Castro-Rubio, F., Marina, M.L., Lindner, W., 2006. Identification of marker proteins for the adulteration of meat products with soybean proteins by multidimensional liquid chromatography-tandem mass spectrometry. J. Proteome Res. 5 (9), 2424–2430. https://doi.org/10.1021/pr060145q.

Liu, K., Ning, M., 2021. Antioxidant activity stability and digestibility of protein from Se-enriched germinated brown rice. LWT - Food Sci. Technol. 142, 111032. https://doi.org/10.1016/j.lwt.2021.111032.

Liu, C., Wang, H., Cui, Z., He, X., Wang, X., Zeng, X., Hao, M., 2007. Optimization of extraction and isolation for 11S and 7S globulins of soybean seed storage protein. Food Chem. 102 (4), 1310–1316. https://doi.org/10.1016/j.foodchem.2006.07.017.

Liu, Y., Zhang, D., Wu, Y., Dan, W., Ji, B., 2014. Stability and absorption of anthocyanins from blueberries subjected to a simulated digestion process. Int. J. Food Sci. Nutr. 65 (4), 440–448. https://doi.org/10.3109/09637486.2013.869798.

Liu, X., Shi, J., Yi, J., Zhang, X., Cai, S., 2020. The effect of in vitro simulated gastrointestinal digestion on phenolic bioaccessibility and bioactivities of Prinsepia utilis Royle fruits. LWT - Food Sci. Technol. (Lebensmittel-Wissenschaft -Technol.) 138 (1), 110782. https://doi.org/10.1016/j.lwt.2020.110782.

Meng, C.Y., Zeng, Y.C., Lin, Y.H., Chen, J., 2017. Effects of L-cysteine and quercetin on the stability of soybean protein isolate(SPI). J. Anhui Agric. Sci. 45 (3), 83–85. https://doi.org/10.13989/j.cnki.0517-6611.2017.03.029.

Munawaroh, H., Gumilar, G.G., Nurjanah, F., Yuliani, G., Show, P.L., 2020. In-vitro molecular docking analysis of microalgae extracted phycocyanin as an anti-diabetic candidate. Biochem. Eng. J. 161, 107666. https://doi.org/10.1016/j.bej.2020.107666.

Ren, S., Giusti, M.M., 2021. The effect of whey protein concentration and preheating temperature on the color and stability of purple corn, grape and black carrot anthocyanins in the presence of ascorbic acid - sciencedirect. Food Res. Int. 144, 110350. https://doi.org/10.1016/j.foodres.2021.110350.

Ren, C., Xiong, W., Li, J., Li, B., 2019. Comparison of binding interactions of cyanidin-3-O-glucoside to β-conglycinin and glycinin using multi-spectroscopic and thermodynamic methods. Food Hydrocolloids 92, 155–162. https://doi.org/10.1016/j.foodhyd.2019.01.053.

Salah, M., Mansour, M., Zogona, D., Xu, X., 2020. Nanoencapsulation of anthocyanins-loaded β-lactoglobulin nanoparticles: characterization, stability, and bioavailability in vitro. Food Res. Int. 137 (3), 109635. https://doi.org/10.1016/j.foodres.2020.109635.

Silveira, R.A.C., Shirley, A., Angelica, M.M., Susanne, T., Giuliana, N., 2021. Dark sweet cherry (Prunus avium) anthocyanins inhibited the growth and biomarkers for breast cancer growth and invasion in highly metastatic 4T1 tumor cells. Curr. Dev. Nutr 5 (279). https://doi.org/10.1093/cdn/nzab036_021.

Sui, X., Sun, H., Qi, B., Zhang, M., Li, Y., Jiang, L., 2018. Functional and conformational changes to soy proteins accompanying anthocyanins: focus on covalent and non-covalent interactions. Food Chem. 245, 871–878. https://doi.org/10.1016/j.foodchem.2017.11.090.

Sun, D., Huang, S., Cai, S., Cao, J., Han, P., 2015. Digestion property and synergistic effect on biological activity of purple rice (Oryza sativa L.) anthocyanins subjected to a simulated gastrointestinal digestion *in vitro*. Food Res. Int. 78, 114–123. https://doi.org/10.1016/j.foodres.2015.10.029.

Valdez, J.C., Bolling, B.W., 2019. Anthocyanins and intestinal barrier function: a review. J. Food Bioact. 5, 18–30. https://doi.org/10.31665/JFB.2019.5175.

Van Der Spoel, D., Lindahl, E., Hess, B., Groenhof, G., Mark, A.E., Berendsen, H.J., 2005. GROMACS: fast, flexible, and free. J. Comput. Chem. 26 (16), 1701–1718. https://doi.org/10.1002/jcc.20291.

Yang, J., Chen, J., Hao, Y., Liu, Y., 2021. Identification of the DPPH radical scavenging reaction adducts of ferulic acid and sinapic acid and their structure-antioxidant activity relationship. LWT - Food Sci. Technol. (Lebensmittel-Wissenschaft -Technol.) 146, 111411. https://doi.org/10.1016/j.lwt.2021.111411.

Zang, Z., Chou, S., Tian, J., Lang, Y., Li, B., 2020. Effect of whey protein isolate on the stability and antioxidant capacity of blueberry anthocyanins: a mechanistic and in vitro simulation study. Food Chem. 336, 127700. https://doi.org/10.1016/j.foodchem.2020.127700.